

# Real-Time Measurement of Oligomeric Species in Secondary Organic Aerosol with the Aerosol Time-of-Flight Mass Spectrometer

Deborah S. Gross,<sup>\*,†</sup> Markus E. Gälli,<sup>‡</sup> Markus Kalberer,<sup>§</sup> Andre S. H. Prevot,<sup>||</sup> Josef Dommen,<sup>||</sup> M. Rami Alfarra,<sup>||</sup> Jonathan Duplissy,<sup>||</sup> Kathrin Gaeggeler,<sup>||</sup> Astrid Gascho,<sup>||</sup> Axel Metzger,<sup>||</sup> and Urs Baltensperger<sup>||</sup>

Department of Chemistry, Carleton College, 1 North College Street, Northfield, Minnesota 55057, TSI Inc., 500 Cardigan Road, Shoreview, Minnesota 55126, Department of Chemistry and Applied Biosciences, ETH Zurich, 8093 Zurich, Switzerland, and Laboratory of Atmospheric Chemistry, Paul Scherrer Institut, 5232 Villigen PSI, Switzerland

Real-time detection of oligomers in secondary organic aerosols has been carried out with an aerosol time-of-flight mass spectrometer sampling particles generated in a smog chamber. The photooxidation products of 1,3,5-trimethylbenzene and NO<sub>x</sub> were studied over a range of initial 1,3,5-trimethylbenzene concentrations (137–1180 ppb), while keeping the 1,3,5-trimethylbenzene to NO<sub>x</sub> ratio nearly constant. The photooxidation products of a mixture of  $\alpha$ -pinene (initial concentration 191 ppb), 1,3,5-trimethylbenzene (60 ppb), and NO<sub>x</sub> were also investigated. In both systems, ions were observed in the single-particle mass spectra up to 750 Da; the species observed differed in the two systems. These high-mass ions occur with characteristic spacing of 14 and 16 Da, indicative of oligomeric species. The results obtained agree well with off-line (matrix-assisted) laser desorption/ionization mass spectrometry results. The real-time capabilities of the aerosol time-of-flight mass spectrometer make it possible to investigate the temporal development of the oligomers with 5-min time resolution and also demonstrate that there are certain ions within the oligomer population that occur in nearly all of the particles and with relatively high signal intensity, suggesting that these ions have higher stability or that the species are formed preferentially.

Secondary organic aerosol (SOA) is composed of a variety of chemical compounds that are formed by reactions of gas-phase precursors and that then form aerosol particles. The chemical identity of the components of SOA can be difficult to determine in complex ambient aerosol, due to the diversity of compounds, the difficulty of sampling the compounds, and their complex chemical structure. A detailed understanding of the chemical

composition of SOA is important to achieve, both to better understand the processes that are occurring in the ambient atmosphere as well as to better describe SOA in atmospheric models. Recent work has highlighted the importance of oligomeric molecules within SOA.<sup>1–13</sup> The existence of oligomers in SOA has significant implications for the physical behavior of the SOA particles in the atmosphere, as well as for their behavior in atmospheric models.

Kalberer et al. and Baltensperger et al.<sup>5,8,9</sup> showed that high-mass oligomers, up to ~1000 Da, can be detected by (matrix-assisted) laser desorption/ionization mass spectrometry ((MA)-LDI-MS) when SOA is generated by reaction of NO<sub>x</sub> with either 1,3,5-trimethylbenzene (TMB),  $\alpha$ -pinene, or isoprene under controlled photooxidation conditions in a smog chamber. Samples were collected on impactor substrates. Subsequent off-line mass spectral analysis showed the presence of a distribution of species with molecular masses up to ~1000 Da, with the characteristic spacing between the peaks of 14, 16, or 18 Da.

- (1) Hoffmann, T.; Bandur, R.; Hoffmann, S.; Warscheid, B. *Spectrochim. Acta, Part B* **2002**, *57*, 1635–1647.
- (2) Ziemann, P. J. *J. Phys. Chem. A* **2002**, *106*, 4390–4402.
- (3) Tolocka, M. P.; Jang, M.; Ginter, J. M.; Cox, F. J.; Kamens, R. M.; Johnston, M. V. *Environ. Sci. Technol.* **2004**, *38*, 1428–1434.
- (4) Iinuma, Y.; Böge, O.; Gnauk, T.; Herrmann, H. *Atmos. Environ.* **2004**, *38*, 761–773.
- (5) Kalberer, M.; Paulsen, D.; Sax, M.; Steinbacher, M.; Dommen, J.; Prevot, A. S. H.; Fisseha, R.; Weingartner, E.; Frankevich, V.; Zenobi, R.; Baltensperger, U. *Science* **2004**, *303*, 1659–1662.
- (6) Gao, S.; Keywood, M.; Ng, N. L.; Surratt, J.; Varutbangkul, V.; Bahreini, R.; Flagan, R. C.; Seinfeld, J. H. *J. Phys. Chem. A* **2004**, *108*, 10147–10164.
- (7) Gao, S.; Ng, N. L.; Keywood, M.; Varutbangkul, V.; Bahreini, R.; Nenes, A.; He, J. W.; Yoo, K. Y.; Beauchamp, J. L.; Hodyss, R. P.; Flagan, R. C.; Seinfeld, J. H. *Environ. Sci. Technol.* **2004**, *38*, 6582–6589.
- (8) Baltensperger, U.; Kalberer, M.; Dommen, J.; Paulsen, D.; Alfarra, M. R.; Coe, H.; Fisseha, R.; Gascho, A.; Gysel, M.; Nyeki, S.; Sax, M.; Steinbacher, M.; Prevot, A. S. H.; Sjögren, S.; Weingartner, E.; Zenobi, R. *Faraday Discuss.* **2005**, *130*, 265–278.
- (9) Kalberer, M.; Sax, M.; Samburova, V. Submitted to *Environ. Sci. Technol.*
- (10) Zahardis, J.; LaFranchi, B. W.; Petrucci, G. A. *Atmos. Environ.* In press.
- (11) Dreyfus, M. A.; Tolocka, M. P.; Dodds, S. M.; Dykins, J.; Johnston, M. V. *J. Phys. Chem. A* **2005**, *109*, 6242–6248.
- (12) Liggio, J.; Li, S.-M.; McLaren, R. *Environ. Sci. Technol.* **2005**, *39*, 1532–1541.
- (13) Bahreini, R.; Keywood, M. D.; Ng, N. L.; Varutbangkul, V.; Gao, S.; Flagan, R. C.; Seinfeld, J. H.; Worsnop, D. R.; Jimenez, J. L. *Environ. Sci. Technol.* **2005**, *39*, 5674–5688.

\* To whom correspondence should be addressed. E-mail: dgross@carleton.edu. Telephone: +1 507-646-5629. Fax: +1 507-646-4400.

<sup>†</sup> Carleton College.

<sup>‡</sup> TSI Inc.

<sup>§</sup> ETH Zurich.

<sup>||</sup> Paul Scherrer Institute.

Similar results have been found by other researchers for a variety of other SOA systems, including  $\alpha$ -pinene ozonolysis products,<sup>3,4,6</sup> and the ozonolysis of a variety of hydrocarbon precursors.<sup>7,10</sup> These oligomers are formed both in the presence of acidic seed particles and in their absence. Gao et al.<sup>6,7</sup> used off-line mass spectrometry to investigate oligomeric compounds formed from many organic precursor molecules, both with and without seed particles. Oligomeric species up to 1600 Da were detected with electrospray ionization (ESI) in an ion trap mass spectrometer. Sulfuric acid seed particles were found to promote the formation of oligomeric species. Tolocka et al.<sup>3</sup> used ESI and matrix-assisted laser desorption/ionization (MALDI) to investigate the oligomeric species detected from the ozonolysis of  $\alpha$ -pinene in the presence of acidic seed particles and determined from exact mass measurements that there are complex reaction mechanisms responsible for the formation of some of the oligomeric species.

In addition to the laser-based ionization methods and ESI, the oligomers in SOA have been detected with photoionization aerosol mass spectrometry,<sup>11,14</sup> with atmospheric pressure chemical ionization,<sup>1</sup> and with photoelectron resonance capture ionization aerosol mass spectrometry.<sup>10,15</sup> Thermal desorption particle beam mass spectrometry has shown the presence of species with lower volatility than dicarboxylic acids from the reaction of cyclic alkenes with ozone, which are attributed to diacyl peroxides.<sup>2</sup> SOA from a variety of precursors has been monitored in real time with the aerosol mass spectrometer,<sup>12,13</sup> which utilizes thermal desorption of particles and electron impact ionization, but in these experiments ions were detected only up to 200 Da, significantly below the typical mass range of the oligomers detected with other techniques. The combination of all of these studies conclusively demonstrates the presence of the high-mass oligomeric species in laboratory systems. High-mass species (oligomers, macromolecules) have also been observed in ambient samples using both on-line<sup>16</sup> and off-line<sup>3,8,17</sup> mass spectrometry. It is of interest to measure the formation of these species in a smog chamber with a real-time, on-line method, to better understand the mechanisms for their formation as well as their implications in atmospheric chemistry.

The aerosol time-of-flight mass spectrometer (ATOFMS) is an instrument designed to sample single aerosol particles in real time.<sup>18,19</sup> Using laser desorption/ionization, the positive and negative ions generated from a single aerosol particle are detected with a bipolar time-of-flight mass spectrometer, generating two complete mass spectra from each individual particle. This instrument is routinely used for sampling ambient atmospheric aerosols and has been used in many other applications. The commercial version of this instrument is designed to efficiently detect ions below  $\sim 300$  Da, and the efficiency of ion transmission has been shown to decrease significantly for larger ions.<sup>20</sup>

In this work, we use the ATOFMS to investigate the formation of SOA from the photooxidation of TMB and  $\alpha$ -pinene (with a small amount of TMB added; see below) in the presence of  $\text{NO}_x$ , in the smog chamber at the Paul Scherrer Institute.<sup>21</sup> The precursors chosen are representative of anthropogenic (TMB) and biogenic ( $\alpha$ -pinene) species found in the atmosphere. A close examination of the single-particle mass spectra generated from the SOA particles shows a clear signature of oligomeric species, with the characteristic spacing of 14 or 16 Da. In this paper, we describe the particles detected and compare the peaks detected with the ATOFMS with those detected by off-line techniques. In addition, the time development of the relatively high mass oligomeric species is discussed in a qualitative manner.

## EXPERIMENTAL SECTION

**PSI Smog Chamber.** The Paul Scherrer Institute smog chamber has been described in detail elsewhere.<sup>21</sup> Briefly, it is a 27-m<sup>3</sup> Teflon bag (3m  $\times$  3m  $\times$  3m) enclosed in a thermally regulated structure. The chamber is illuminated with four 4-kW xenon arc lamps, to simulate the tropospheric solar spectrum. The lights are turned on after the gaseous precursors are equilibrated in the chamber (typically 30–60 min). Experiments were monitored with a variety of aerosol and gas-phase characterization instruments, including a CPC (TSI 3025a), SMPS (TSI 3071 and 3010 CPC), VTDMA, real-time monitors for gas-phase  $\text{O}_3$ ,  $\text{NO}$ , and  $\text{NO}_2$ , and a PTR-MS (Ionicon Analytic GmbH). All experiments described here were conducted at  $\sim 50\%$  relative humidity, and no seed particles were added in any experiments.

**Single-Particle Mass Spectrometry.** The aerosol time-of-flight mass spectrometer (TSI 3800, Shoreview, MN) is a single-particle mass spectrometer designed to sample individual aerosol particles in real time.<sup>18,19</sup> Particle-laden air is sampled through a convergent nozzle at 0.85 L/min. The particles and the gas are accelerated, and the particles attain a terminal velocity that is proportional to their aerodynamic diameter ( $D_a$ ). After two stages of differential pumping, the particle  $D_a$  is determined by measuring the time between pulses of scattered light as the particle passes through two continuous wave diode pumped Nd:YAG lasers (532 nm, CrystaLaser, Reno, NV) located a known distance apart. From this, the particle's velocity is calculated, and this value is used to synchronize the particle's arrival time in the source of the bipolar time-of-flight mass spectrometer with a pulse of the fourth harmonic of a Nd:YAG laser, used for desorption and ionization of the particles (266 nm,  $\sim 1$  mJ/pulse,  $1 \times 10^8$  W/cm<sup>2</sup>, Big Sky Laser, Bozeman, MT). The interaction of the particle with the laser beam generates both positive and negative ions, which are accelerated into the respective flight tubes of the instrument. Thus, from each particle that successfully interacts with the desorption/ionization laser, complete positive and negative ion mass spectra are generated. The  $D_a$  and sampling time of each particle is recorded as well.

The ATOFMS instrument sampled directly from the PSI smog chamber, through a 0.25-in.-o.d. coated stainless steel sampling

- (14) Öktem, B.; Tolocka, M. P.; Johnston, M. V. *Anal. Chem.* **2004**, *76*, 253–261.
- (15) Zahardis, J.; LaFranchi, B. W.; Petrucci, G. A. *J. Geophys. Res.* **2005**, *110*, D08307; DOI: 10.1029/2004JD005336.
- (16) Prather, K. A., University of California, San Diego, personal communication, 2005.
- (17) Kiss, G.; Tombácz, E.; Varga, B.; Alsberg, T.; Persson, L. *Atmos. Environ.* **2003**, *37*, 3783–3794.
- (18) Noble, C. A.; Prather, K. A. *Environ. Sci. Technol.* **1996**, *30*, 2667–2680.
- (19) Gard, E. E.; Mayer, J. E.; Morrical, B. D.; Dienes, T.; Fergenson, D. P.; Prather, K. A. *Anal. Chem.* **1997**, *69*, 4083–4091.

- (20) Czerwieniec, G. A.; Russell, S. C.; Lebrilla, C. B.; Coffee, K. R.; Riot, V.; Steele, P. T.; Frank, M.; Gard, E. E. *J. Am. Soc. Mass Spectrom.* **2005**, *16*, 1866–1875.
- (21) Paulsen, D.; Dommen, J.; Kalberer, M.; Prévôt, A. S. H.; Richter, R.; Sax, M.; Steinbacher, M.; Weingartner, E.; Baltensperger, U. *Environ. Sci. Technol.* **2005**, *39*, 2668–2678.

**Table 1. Experimental Conditions for Smog Chamber Experiments, Including the Total Number of Particles Sampled with the ATOFMS in Each Experiment**

| expt | [TMB]<br>(ppb) | [ $\alpha$ -pinene]<br>(ppb) | [NO]<br>(ppb) | [NO <sub>2</sub> ]<br>(ppb) | [VOC]/[NO <sub>x</sub> ] | RH<br>(%) | expt<br>duration<br>(hh:mm) |
|------|----------------|------------------------------|---------------|-----------------------------|--------------------------|-----------|-----------------------------|
| 1    | 137            | 0                            | 0             | 65                          | 2.1                      | 48        | 8:50                        |
| 2    | 560            | 0                            | 129           | 141                         | 2.1                      | 52        | 26:11                       |
| 3    | 1137           | 0                            | 300           | 343                         | 1.8                      | 46        | 8:35                        |
| 4    | 1180           | 0                            | 535           | 0                           | 2.2                      | 49        | 8:36                        |
| 5    | 1171           | 0                            | 330           | 313                         | 1.8                      | 49        | 8:45                        |
| 6    | 60             | 191                          | 57            | 76                          | 1.4                      | 51        | 8:41                        |

line (Sulfinert, Restek Inc.). ATOFMS sampling typically began either at the time the lights were turned on in the chamber or at the time when particle nucleation was detected by the SMPS. The ATOFMS with the nozzle inlet samples particles in the 150 nm–3  $\mu$ m size range and thus was not able to detect freshly nucleated particles. In the experiments described here, particles grew into the relevant size range within 1–2 h. Experiments lasted either  $\sim$ 8 or  $\sim$ 24 h after lights were turned on (see Table 1) and the ATOFMS sampled continuously.

The ATOFMS instrument, sampling through the nozzle inlet used here, is known to have size-dependent transmission of particles into the instrument.<sup>22</sup> The transmission and detection for smaller particles is significantly less efficient than that for larger particles. The function that describes this size dependence has been characterized for this instrument, but we have not applied it to the results presented here, as we are interested in comparing the mass spectral characteristics between experiments, rather than determining the particle concentration.

All instrument settings, including desorption/ionization laser energy, mass spectrometer voltage settings, and particle detection settings, were identical to those used routinely with this instrument for ambient measurements. No unusual instrumental conditions were required to detect the species shown here.

A very small number of particles (on average 1 cm<sup>-3</sup> as determined by the CPC) were detected in the smog chamber prior to particle nucleation and growth into the size range detectable with the ATOFMS. These particles, detected by the ATOFMS on the order of 0–1 every 10 min (compared to 20–60/min, after particle nucleation) constitute the background for these measurements and are readily identifiable by their distinct chemical composition. Blank experiments (without addition of NO<sub>x</sub> and VOC) were not performed with this instrument. However, regular blank experiments in the smog chamber yield a total mass concentration of typically less than 0.5  $\mu$ g/m<sup>3</sup>, with a geometric mean diameter of less than 50 nm. These particles are thus below the detectable size range of the ATOFMS.

**ATOFMS Data Analysis.** In contrast to ambient measurements, the particles in the smog chamber have a highly homogeneous source. Thus, the individual particle mass spectra can be averaged without presorting the particles, to increase the signal-to-noise level of the spectra. In the results shown here, particles are averaged in 5-min and 1-h intervals. The oligomeric species

of interest are detected in low-intensity peaks at relatively high molecular weight (for the TSI 3800 ATOFMS). To be considered a real peak, rather than noise, the peak must have height greater than 5 units, area greater than 6 square units, and contribute more than  $1 \times 10^{-3}\%$  of the total peak area in the spectrum. Typically, the peak area criterion has the most impact on the identification of peaks, and these settings correspond to a 3:1 signal-to-noise ratio in individual particle spectra, with the noise being primarily electronic. For analysis of ambient data, we use peak criteria that are approximately twice that used in these experiments, to minimize the contribution from very small peaks and to simplify analysis. In all experiments described here, peak detection was carried out up to  $\pm 750$  Da.

#### Off-Line Laser Desorption/Ionization Mass Spectrometry.

Sampling and analysis methods for the off-line mass spectrometric methods are described in detail elsewhere.<sup>5,9</sup> Briefly, TMB SOA particles were sampled on uncoated impactor plates for 1–4 h. After sampling, the TMB SOA was directly measured without further preparation. The  $\alpha$ -pinene SOA was sampled onto impactor plates coated with graphite particles. Both samples were analyzed using a TOF-MS (Axima-CFR, Kratos/Shimadzu, Manchester, U.K.) measuring in the positive ion mode. Laser desorption was carried out with a nitrogen laser, operating at 337 nm.

## RESULTS AND DISCUSSION

**On-Line Detection of Oligomeric Species.** The single-particle mass spectra obtained with the ATOFMS at the Paul Scherrer Institute smog chamber contain ion signatures due to oligomeric species. These are the first reported on-line and real-time mass spectrometric measurements of species up to 750 Da in aerosol particles. Figures 1 and 2 (described in detail below) show average mass spectra from two different experiments, with TMB and mixed  $\alpha$ -pinene/TMB precursors, respectively. In general, the spectra contain high-mass peaks, in clusters separated by 14–16 Da, which are consistent with oligomers. The groups of peaks that are separated by 14–16 Da are typically 6 Da wide. These complex spectra suggest that there are multiple overlapping distributions of oligomers rather than a single species. There is also a broader structure in the ion intensity distribution, which we discuss below.

The oligomer peaks in the SOA generated from TMB were detected in multiple experiments. The details of these experiments, including initial concentrations of the precursor organic compound and all other added gases, are shown in Table 1. In all TMB experiments, the [TMB] to [NO<sub>x</sub>] ratio was initially close to 2, and the relative humidity was  $\sim$ 50%. The different initial [NO<sub>2</sub>] to [NO] ratios should not influence particle composition since particle formation occurs only after [NO] reaches low levels in all these experiments. One experiment (experiment 6) was conducted with  $\alpha$ -pinene as the organic precursor, spiked with TMB at a level estimated to produce no more than 5% of the SOA mass, based on the yields obtained in this chamber in previous experiments (i.e., 60 ppb TMB is estimated to yield 8  $\mu$ g/m<sup>3</sup> SOA, assuming that the total SOA concentration of 210  $\mu$ g/m<sup>3</sup> is relevant for the TMB SOA partitioning). TMB was added to enhance the detection of the resulting SOA by the ATOFMS, which is unable to ionize the particles formed from the direct photooxidation of  $\alpha$ -pinene under these conditions. This is either due to poor absorption of the 266-nm ionization laser wavelength by the

(22) Allen, J. O.; Fergenson, D. P.; Gard, E. E.; Hughes, L. S.; Morrical, B. D.; Kleeman, M. J.; Gross, D. S.; Gälli, M. E.; Prather, K. A.; Cass, G. R. *Environ. Sci. Technol.* **2000**, *34*, 211–217.



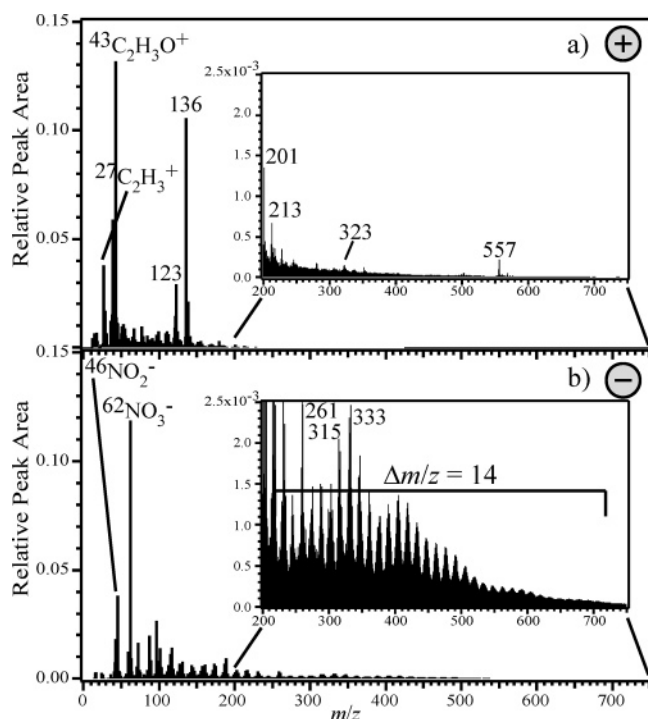


**Figure 1.** Average ATOFMS mass spectra of (a) positive ions and (b) negative ions from the 71 051 particles detected during experiment 2 (1,3,5-trimethylbenzene initial concentration of 560 ppb). The insets show the region from 200 to 750 Da and clearly show the oligomeric ions in the negative mass spectrum.

particles formed from the photooxidation of  $\alpha$ -pinene or to inefficient ionization of desorbed species in the laser desorption/ionization step. The addition of the aromatic species enhances the absorption and subsequent ionization. Similar results have been observed with off-line LDI-MS analyses: SOA oligomers from TMB were observed without any matrix addition, but for  $\alpha$ -pinene and isoprene SOA, matrix addition was necessary to yield sufficient signal intensity.<sup>9</sup>

The ATOFMS instrument detects both positive and negative ions from each particle. The information contained in each polarity spectrum is significantly different, as observed in these experiments. Typically, with the TMB precursor, mostly low-mass (<200 Da) organic fragment ions were observed in the positive ion mass spectrum. The negative ion mass spectrum contains nitrite and nitrate ions ( $\text{NO}_2^-$ ,  $m/z$  -46 and  $\text{NO}_3^-$ ,  $m/z$  -62), low-mass fragments, and organic ions, many of which are consistent with organic acids detected by IC-MS in similar experiments,<sup>23</sup> as well as the high-mass oligomeric ions. Figure 1 shows an average of all 71 051 particle spectra detected in experiment 2, illustrating the differences in the ions detected in the positive and negative ion mass spectra. The insets in the positive and negative ion spectra, which show the mass range from 200 to 750 Da, clearly illustrate the presence of oligomeric species in the negative ion mass spectrum, at masses up to 750 Da. The presence of these peaks only in the negative spectrum suggests acid functionalities in these species. Figure 2 shows the average of all 34 159 particles from experiment 6, which contained primarily  $\alpha$ -pinene as precursor,

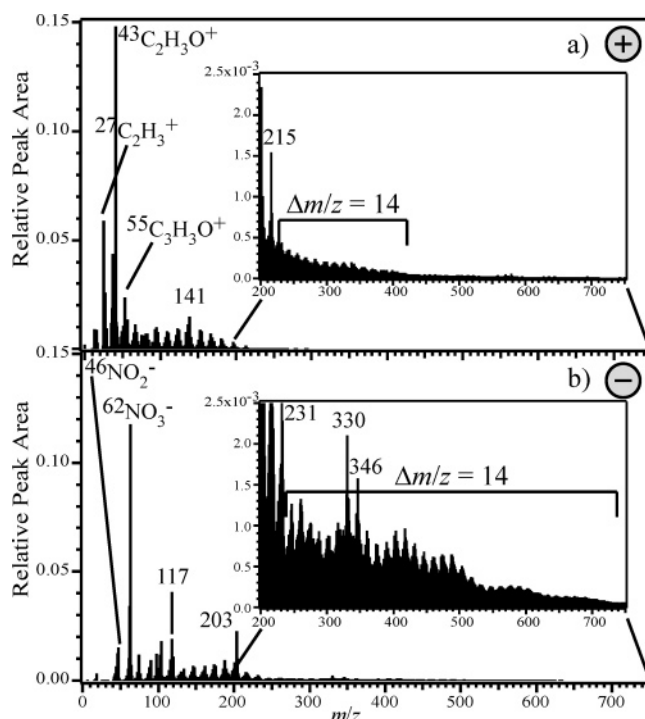


**Figure 2.** Average ATOFMS mass spectra of (a) positive ions and (b) negative ions from the 34 159 particles detected during experiment 6 ( $\alpha$ -pinene initial concentration of 191 ppb and 1,3,5-trimethylbenzene initial concentration of 60 ppb). The insets show the region from 200 to 750 Da and clearly show the oligomeric ions in both the positive and negative mass spectra.

with a small amount of TMB added. The spectra shown in Figure 2 are distinct from those shown in Figure 1, suggesting that the interaction between the small amount of TMB and the  $\alpha$ -pinene, while enough to make it possible to detect the resulting SOA, did not dominate the chemistry in this system. In general, the results are similar to those observed with TMB, in that the positive ion mass spectrum consists primarily of organic fragment ions, but it also contains low-intensity oligomeric species decreasing in relative intensity up to  $\sim 400$  Da. As with the TMB system, the higher mass oligomeric ions are detected in the negative ion mass spectrum. The oligomeric peaks in the TMB system and in the  $\alpha$ -pinene/TMB system occur at different  $m/z$  values, as illustrated by the spectra in Figure 3, which shows an overlay of the 470–500-Da range of the mass spectra, illustrating that they are not identical. This is consistent with different monomer units as building blocks for the higher mass species.

As shown in Table 1, we carried out multiple experiments with TMB as the organic precursor, with a variety of initial concentrations. In all of these experiments, the high-mass oligomeric peaks were observed at the same  $m/z$  values, with similar distributions of relative peak intensity. This is shown in Figure 4, which overlays the mass range of 350–550 Da from the average of all SOA particles detected in experiments 1–5. The peaks appear at the same  $m/z$  values in all of these spectra and are distinct from those observed in the  $\alpha$ -pinene/TMB system, as shown in Figure 3. There is a difference in the relative intensity of the peaks from each experiment, defined as the individual peak area divided by the total area in the spectrum, in general following the trend that higher initial TMB concentrations lead to lower relative intensity of high-mass oligomer ions. This is consistent with the observation

(23) Fisseha, R.; Dommen, J.; Sax, M.; Paulsen, D.; Kalberer, M.; Maurer, R.; Höfler, F.; Weingartner, E.; Baltensperger, U. *Anal. Chem.* **2004**, *76*, 6535–6540.

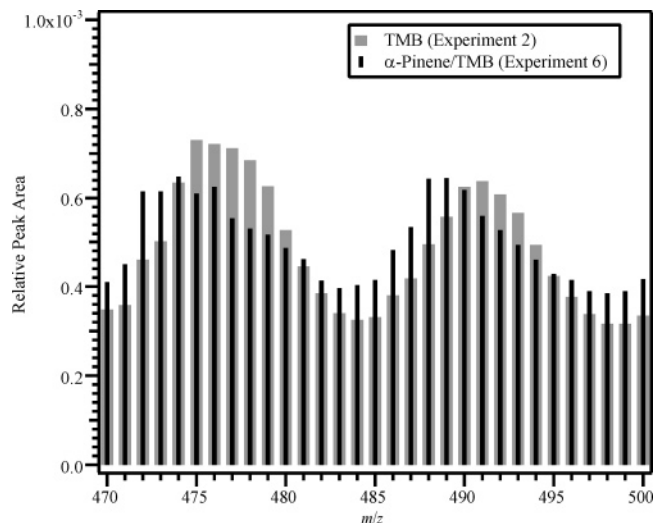


**Figure 3.** Overlay of the 470–500-Da mass range from the TMB system (experiment 2), shown in gray, and the  $\alpha$ -pinene/TMB system (experiment 6), shown in black, illustrating that the peak positions for the oligomer peaks are not identical in these two systems.

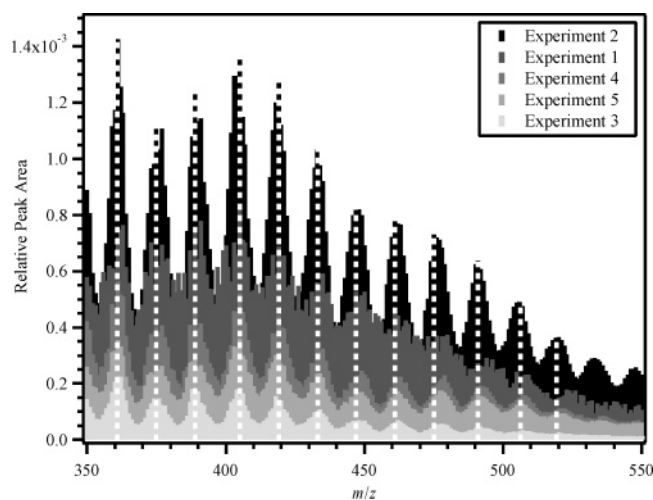


**Figure 4.** Overlay of the 350–550-Da region of the ATOFMS negative ion mass spectra from experiments 1–5 (1,3,5-trimethylbenzene precursor, see Table 1 for initial concentrations), showing the reproducibility of the oligomer peaks. Vertical dotted lines are inserted to guide the eye.

that SOA formed at lower initial TMB concentrations was less volatile than SOA formed from higher TMB concentrations.<sup>5</sup>

The peaks observed from the precursors studied here also match up well with those detected using off-line (MA)LDI-MS. Figure 5a shows LDI-MS results obtained for TMB SOA in the positive ion mode overlaid with a reconstructed average ATOFMS negative ion mass spectrum from experiment 2. Figure 5b shows MALDI-MS results obtained for  $\alpha$ -pinene SOA in the positive ion mode overlaid with a reconstructed average ATOFMS negative ion mass spectrum from experiment 6. Because LDI-MS generates positive  $[M + K]^+$  pseudomolecular ions<sup>5</sup> while we assume that the ATOFMS negative ion spectra are  $[M - H]^-$  pseudomolecular ions,<sup>24</sup> we cannot compare the peak positions directly. Instead, the  $m/z$  axis for the ATOFMS spectra shown in Figure 5 are shifted by the addition of 40 Da, to correspond with that of the

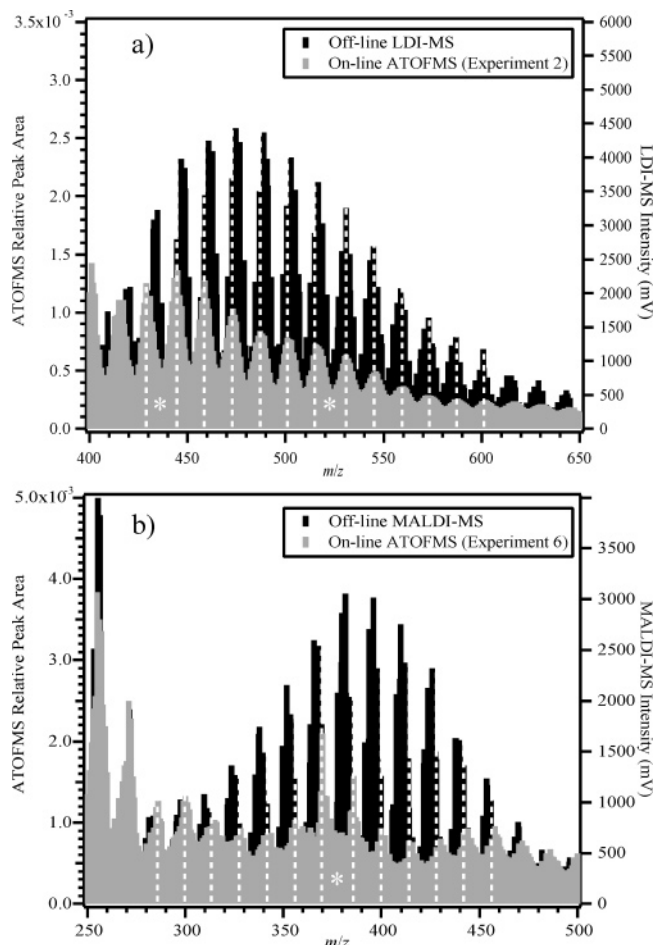


**Figure 5.** Overlay of on-line ATOFMS average mass spectrum and off-line (MA)LDI-MS mass spectra for (a) 1,3,5-trimethylbenzene SOA and (b)  $\alpha$ -pinene SOA (MALDI-MS) and  $\alpha$ -pinene/TMB SOA (ATOFMS). Because the off-line (MA)LDI-MS detects positive ions as  $K^+$  adducts, while the ATOFMS detects deprotonated negative ions, the ATOFMS spectra have been transformed by the addition of 40 Da to the original mass scale for this overlay. Vertical lines have been added at increments of 14 Da to guide the eye (except for the instances marked with an asterisk (\*), where the lines are 16 Da apart).

(MA)LDI-MS spectrum (i.e.,  $[M - H]^- + 40 = [M + K]^+$ ). While there is not perfect overlap between the two spectra from each precursor, the agreement is overall quite good. The most striking similarity is in the overlap of peak  $m/z$  values, while the greatest difference is in the intensity distributions of the peaks. The  $m/z$  overlap appears slightly better in the TMB system (Figure 5a) than in the  $\alpha$ -pinene/TMB system (Figure 5b). This small difference is presumably due to the addition of TMB in the ATOFMS experiment, while the MALDI-MS results were obtained from a pure  $\alpha$ -pinene system.

In both the TMB and the  $\alpha$ -pinene/TMB experiments discussed here, there are certain ions that stand out above the oligomer distribution at masses greater than  $\sim 200$  Da in the mass spectra, with peaks of higher intensity than at nearby  $m/z$  values. These higher intensity ions are different in the TMB and  $\alpha$ -pinene/TMB experiments and are likely due to the different monomers that are formed from the photochemical reactions of these precursors—either their preferential formation or their enhanced ion stability. Their mass-to-charge values are labeled

(24) Silva, P. J.; Prather, K. A. *Anal. Chem.* **2000**, *72*, 3553–3562.

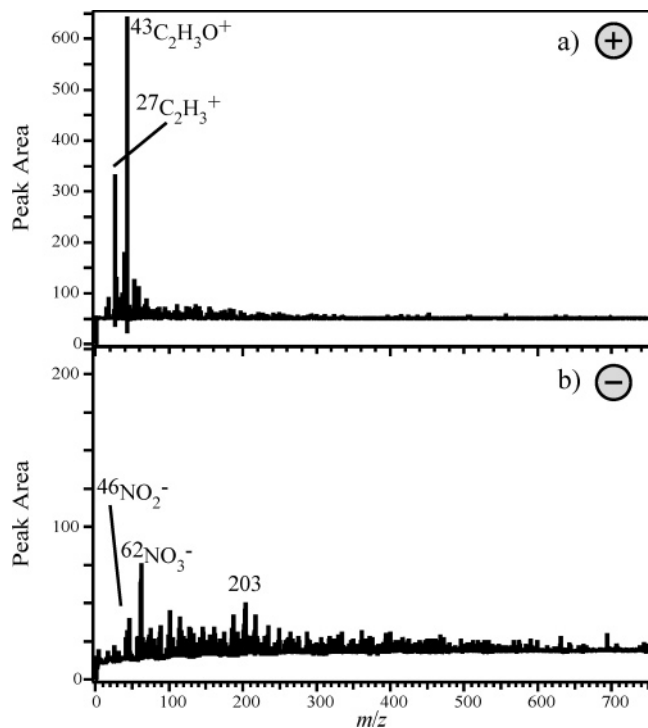


**Figure 6.** ATOFMS mass spectrum from a single particle detected in experiment 6, showing both (a) positive ions and (b) negative ions.

in the spectra shown in Figures 1 and 2. The identities of these peaks are currently under investigation.

**Time Development of Oligomeric Species.** The advantage of the ATOFMS instrument is that it obtains mass spectra from particles in real time. Because the peaks due to the high-mass

oligomeric species are of very low intensity, they are not easily discerned in individual spectra, although they can be seen at low intensity in the spectrum of individual particles, such as that shown in Figure 6. Any given high-mass oligomer peak is found in between 20 and 70% of single-particle mass spectra, while the higher intensity peaks labeled in Figures 1 and 2 appear in nearly 100% of the single-particle spectra. Thus, averaging particles together is both necessary and possible for the more detailed analysis carried out here. Here we average particles on a time basis, both in long (1 h) and short (5 min) time bins, to illustrate the development of the oligomeric species over the course of the experiments. In all cases, time is expressed as time since the lights in the smog chamber were turned on, initiating the photochemical degradation of the organic precursors.

The peaks observed in the 250–750-Da range in all of the spectra obtained in these experiments evolve over the course of the experiment (see Table 1 for experiment durations). Figure 7 shows the time development of the negative ion mass spectra observed from experiment 6, in 1-h time bins. The high-mass species observed can be seen in the second hour after the lights are turned on, but they continue to develop over the course of the experiment. Figure 8 shows the 250–650-Da range from experiment 6 with 5-min time resolution rather than 1 h. These data emphasize the fact that real-time changes in the relative peak intensity and molecular weight of these oligomeric species can be readily detected with the ATOFMS instrument. As soon as particles are detected with the ATOFMS instrument (within 1–2 h after the chamber lights are turned on to initiate the photochemical reactions, depending on the experimental conditions), there are peaks at masses greater than 400 Da (see Figures 7 and 8). These oligomer ions continue to grow, both in relative

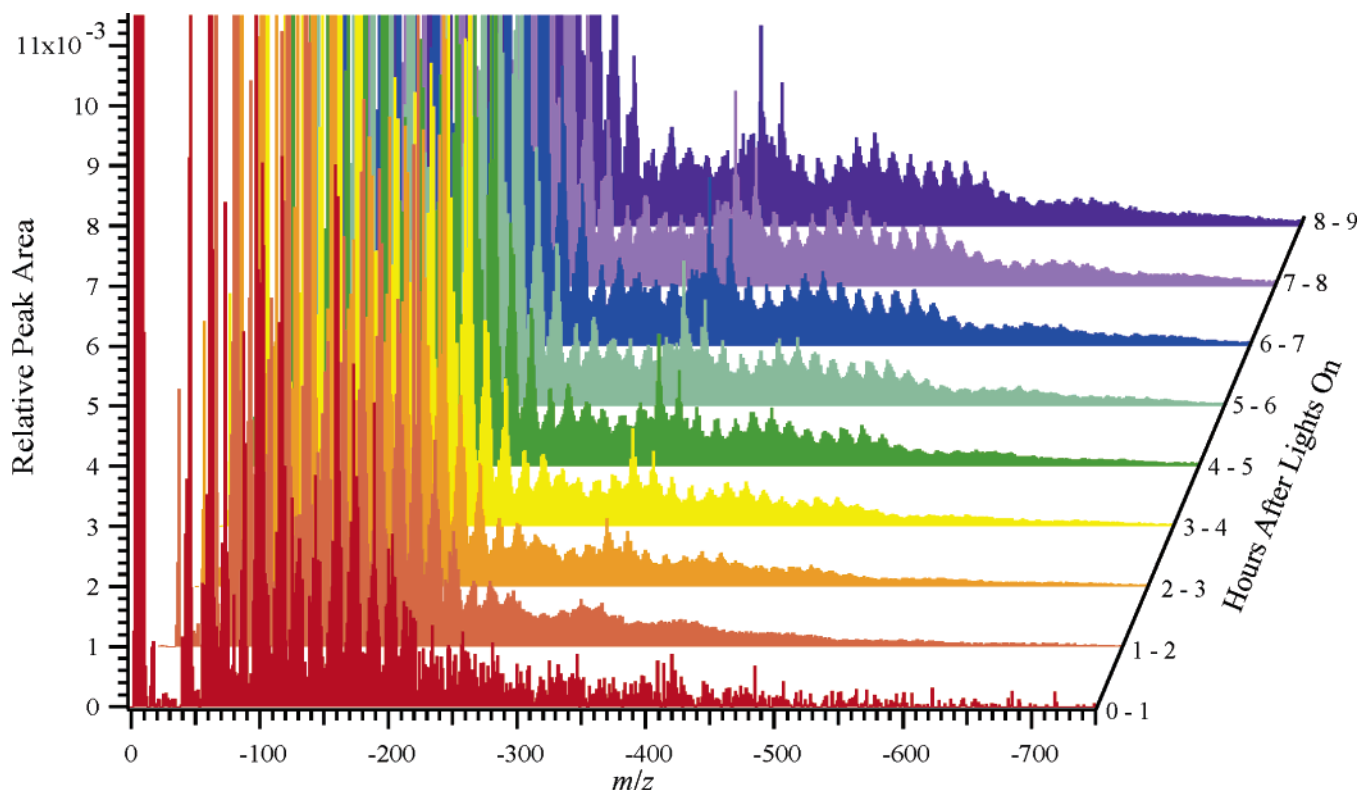


**Figure 7.** Waterfall plot showing the average ATOFMS negative ion mass spectrum for each hour of data after the lights were turned on in experiment 6. Note that the spectra are offset from each other on the x-axis by 20 Da/spectrum, to aid in visualization.

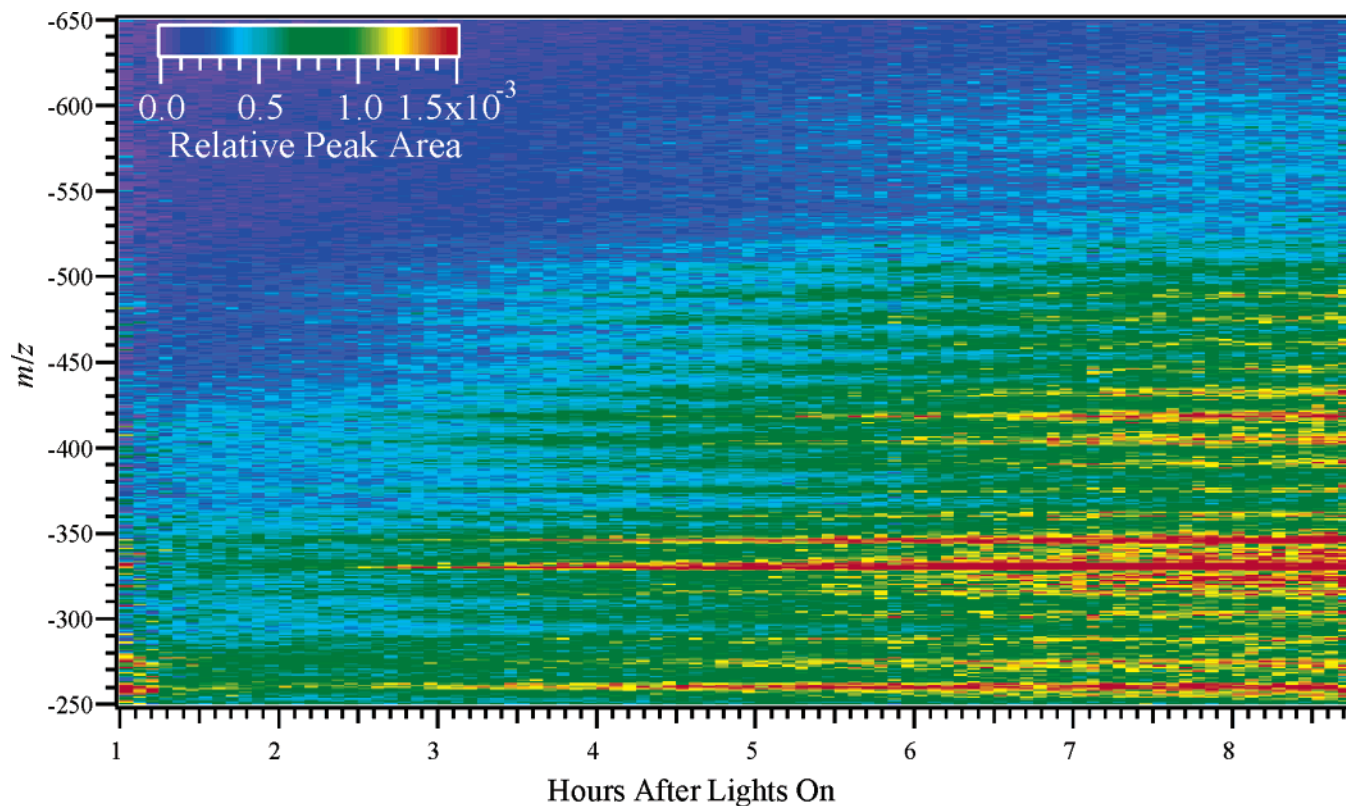


**Figure 8.** Image plot showing the average ATOFMS negative ion mass spectrum for every 5 min of data after the lights were turned on in experiment 6. The y-axis indicates the  $m/z$  value of the ion, and the color of each pixel indicates the relative peak area for that  $m/z$  value. The color scale, which is shown in the figure, is chosen to emphasize the high-mass peaks and therefore severely truncates higher intensity lower mass peaks. The maximum relative peak area in this data set is  $\sim 0.1$ .

peak intensity and in molecular weight, at least for the first 8 h after lights were turned on. Similar results were obtained for the TMB systems studied. Future work will focus on obtaining relative rates for the formation of various ions and mass ranges from this high time-resolution data.

In experiment 6, there are broad maxima and minima in the intensity profiles of the oligomeric species in addition to the 14–16-Da spacing between peaks, as seen in Figures 2, 6, and 7 from the  $\alpha$ -pinene with TMB experiment. In the TMB experiments, the maxima and minima within the profile are more pronounced (see Figure 1). The spacing between these broad maxima (or minima) is  $\sim 75$  Da. The maxima are slightly offset with respect to each other, but the minima are remarkably similar. This is in contrast to the LDI-MS results,<sup>9</sup> which show very different broad peak intensity distributions for the different precursors. These differences result, at least partially, from different ion transmission efficiencies in the instruments. Careful comparison of the ATOFMS ion distributions, as well as the specific ions that appear with higher intensity in each experiment, can be helpful in the analysis of ambient samples obtained with the ATOFMS.

**Particle Size Dependence of Oligomeric Peaks.** One of the features of the ATOFMS instrument is that the size of each sampled particle is measured, as aerodynamic diameter ( $D_a$ ). The size distributions of the particles sampled in these experiments varied, due to the initial concentrations of VOC. The size distributions detected by the ATOFMS show growth of the particles from the initial size that the ATOFMS can detect (typically  $D_a \geq 150$  nm) to the final size distribution. The initial growth rate is rapid, and the number of particles initially detected

**Table 2. Average Raw Aerodynamic Diameter for Particles from Which ATOFMS Mass Spectra Were Obtained<sup>a</sup> and Information about ATOFMS Particle Counts, Particle Number, and Volume Concentrations**

| expt | no. of particles generating ATOFMS mass spectra | av particle size of particles generating ATOFMS mass spectra ( $D_a$ , nm) | peak particle no. concn from the CPC (no./cm <sup>3</sup> ) | particle vol concn calcd from the SMPS ( $\mu\text{m}^3/\text{cm}^3$ ) |
|------|-------------------------------------------------|----------------------------------------------------------------------------|-------------------------------------------------------------|------------------------------------------------------------------------|
| 1    | 4 836 <sup>b</sup>                              | $360 \pm 90$                                                               | 583                                                         | $5.5 \pm 0.5$                                                          |
| 2    | 71 051                                          | $730 \pm 130$                                                              | 550                                                         | $40 \pm 10^c$                                                          |
| 3    | 23 481                                          | $680 \pm 200$                                                              | 1143                                                        | nd <sup>d</sup>                                                        |
| 4    | 14 089                                          | $770 \pm 210$                                                              | 1071                                                        | $130 \pm 13$                                                           |
| 5    | 10 929                                          | $860 \pm 290$                                                              | 721                                                         | nd <sup>d</sup>                                                        |
| 6    | 34 159                                          | $640 \pm 150$                                                              | 3682                                                        | $210 \pm 30^c$                                                         |

<sup>a</sup>As the average  $\pm$  one standard deviation of the best-fit Gaussian for the log-normal size distribution. <sup>b</sup>This experiment included sampling through thermal denuder at various temperatures thus decreasing the overall particle counts. <sup>c</sup>Increased uncertainty due to a small fraction of larger particles outside the measurement range, for which an approximate correction was applied. <sup>d</sup>This value was not determined because a high fraction of particles was outside the measurement range.

by the ATOFMS is relatively low. The growth rate then levels off significantly, resulting in a relatively narrow size distribution. Average particle sizes for the particles hit by the ATOFMS are given for experiments 1–6 in Table 2, along with the peak particle number and volume concentrations detected in these experiments.



We have investigated whether there is any size dependence of the oligomeric peaks detected. For both the TMB and the mixed  $\alpha$ -pinene/TMB system, we looked at average mass spectra for particles in specific size ranges within the particle size distribution for each hour after the lights were turned on. The same size ranges were used for all experiments investigated, and detected particles typically fell within 6–8 size bins (where there are 16 bins per decade, evenly distributed on a log scale), depending on the specific experiment investigated. In these experiments, we observe no size dependence in the particle mass spectra, over the entire mass range investigated. We will continue to investigate this possibility in future experiments.

## CONCLUSIONS

We have demonstrated that the ATOFMS instrument, from which mass spectra of individual particles are obtained, is suitable for on-line detection of oligomeric species formed in SOA, even with its low ion-transfer efficiencies for high-mass ions. The SOA formed from  $\text{NO}_x$ , light, and either TMB or a mixed  $\alpha$ -pinene/TMB precursor in the smog chamber are chemically distinct and likely consist of acidic functional groups, as they are observed in the negative ion mass spectrum preferentially. The mass spectra obtained with the ATOFMS compare well with off-line (MA)LDI-MS analyses of TMB and  $\alpha$ -pinene SOA oligomers. On-line and real-time detection of these species, as demonstrated here for the

first time, is necessary for a more detailed understanding of the dynamics of the oligomerization process, which we will investigate in future work. Additionally, the single-particle approach taken with the ATOFMS instrument makes it clear that the low-intensity, high-molecular weight species observed here are occurring in the same particles as the higher intensity, low-molecular weight peaks that occur in these spectra, which could be due to monomer units. Further characterization of these oligomers will aid in the interpretation of on-line, real-time ambient datasets.

## ACKNOWLEDGMENT

This work was supported by the Swiss National Science Foundation (2169-061393), the ETHZ (TH-10./01-2), and the European Commission (EUROCHAMP, FP6-505968) as well as the European Science Foundation program 'Interdisciplinary Tropospheric Research: from the laboratory to global change', INTROP. We thank René Richter and Günther Wehrle for their assistance with the smog chamber experiments. D.S.G. thanks Carleton College and the Associated Colleges of the Midwest for support.

Received for review January 19, 2006. Accepted February 10, 2006.

AC060138L